

Photoconductivity Spectra of Single-Carbon Nanotubes: Implications on the Nature of Their Excited States

Xiaohui Qiu, Marcus Freitag, Vasili Perebeinos, and Phaedon Avouris*

IBM Research Division, T. J. Watson Research Center,
Yorktown Heights, New York 10598

Received February 3, 2005; Revised Manuscript Received February 9, 2005

ABSTRACT

We have measured the photoconductivity excitation spectra of individual semiconducting carbon nanotubes incorporated as the channel of field-effect transistors. In addition to the pronounced resonance that correlates with the second van Hove transition (E_{22}) in semiconducting carbon nanotubes, a weaker sideband at about 200 meV higher energy is observed. Electronic structure calculations that include electron–phonon coupling indicate that the spectra originate from the simultaneous excitation of an exciton (main resonance) and a C–C bond stretching phonon (sideband). The spectral features are not compatible with an interband interpretation of the excitation involved.

The optical properties of carbon nanotubes (CNTs) are receiving extensive attention. Fluorescence and resonant Raman spectroscopy have emerged as powerful techniques for the characterization of the diameter and chirality of individual CNTs in solutions^{1,2} and on surfaces.³ Furthermore, carbon nanotube field-effect transistors (CNT-FETs) are found to have potential application as both photodetectors⁴ and infrared-light emitters.^{5,6} Despite these developments, an open question remains whether the optical transitions observed are excitonic or interband transitions in nature. Given that CNTs are direct band-gap materials, an interband interpretation implies that the lowest optical transition energy would also give the band-gap of the CNT—one of the most important quantities for semiconducting CNTs. On the other hand, CNTs are one-dimensional (1D) confined materials with a typical diameter of ~ 1 – 2 nm. In such systems the confinement is expected to lead to strong electron–hole interaction and the formation of strongly bound excitons.^{7,8} Indeed, state-of-the-art electronic structure calculations predict the presence of strongly bound excitonic states in small diameter (≤ 0.7 nm) CNTs.^{9,10} A simpler computational scheme that includes the electron–hole interaction and allows calculations on CNTs of any diameter and chirality and in different environments has also been developed.¹¹ This calculation finds significant exciton binding, even in larger diameter CNTs and shows that most of the optical intensity is concentrated on the excitonic transition, not the interband transition. In the exciton picture, the optical transition energy does not correspond to the electrical band-gap of the CNT.

Here we present new experimental evidence for the existence of excitonic states in CNTs. We use photoconductivity excitation spectra of single nanotubes in the region of the E_{22} optical transition. In addition to the main optical transition, we observe a satellite peak at ~ 200 meV higher energy. This sideband is interpreted as involving the excitation of an optical phonon. The line shape of the main optical transition, as well as the satellite peak position, are consistent with the optical absorption spectrum obtained using a tight-binding Bethe–Salpeter calculation of the exciton states that includes electron–phonon coupling. In contrast, inclusion of electron–phonon coupling in the interband transitions does not lead to the appearance of well-defined sidebands.

The experimental setup is similar to that described in ref 4. The single walled carbon nanotubes (~ 1.3 nm average diameter) were produced by the laser-ablation method (Rice University). Carbon nanotube field-effect transistors (CNT-FETs) with channel lengths ranging from 500 nm to 1000 nm were fabricated on a p^+ doped silicon wafer coated with 150 nm of SiO_2 . Titanium and cobalt electrodes were used to form electrical contacts to the nanotubes, and the Si wafer itself was used as a back-gate. The as-produced CNT-FETs typically behave as p-type transistors in an ambient environment.¹²

The steady-state photocurrent of individual CNT-FETs was obtained using a linearly polarized continuous wave Ti:sapphire laser with a tunable range from 720 nm (1.72 eV) to 1000 nm (1.24 eV). Typical laser power intensity on the sample was ~ 1 kW/cm². The semiconducting CNTs were excited at the energy of the second optical transition (E_{22}). This state decays and dissociates into free electron–hole pairs

* E-mail: avouris@us.ibm.com.

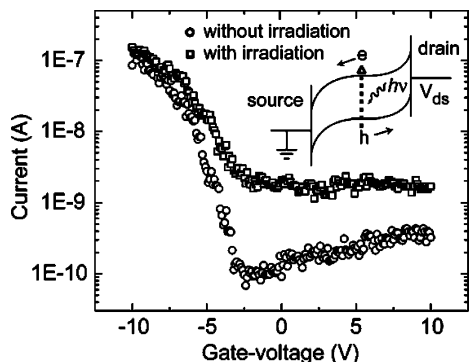


Figure 1. Gate-voltage dependence of the drain current of a CNT-FET with and without laser illumination. The drain voltage was -1.0 V, while the gate voltage was ramped from -10 to 10 V. Inset: Schematic band diagram of a CNT-FET with the gate voltage set at approximately $1/2V_{ds}$. The carriers, electrons and holes, generated by the above-band-gap optical excitation in the nanotube channel are subsequently separated by the external electric field and collected at the two opposite electrodes.

in the first quasi-particle band under the applied external electric field.⁴ The photoconductivity spectra presented in this study are normalized to constant incident photon flux.

Figure 1 shows the gate voltage dependence of the source–drain current of a CNT-FET and its response to laser irradiation. The increase in the OFF-state current of the device upon illumination is due to the charge carriers created in the nanotube by optical excitation and subsequently separated by the applied electric field,^{4,13} as illustrated in the schematic band diagram in Figure 1. In addition to the photocarriers generated in nanotubes, laser irradiation also produces a photovoltage at the interface between SiO_2 and p^+ Si substrate that leads to a shift in the gate-voltage characteristics.⁴ The photocurrent measurements were always carried out well in the OFF-state of the device, where the shift does not affect the current. Compared to ambipolar devices used in previous work,⁴ the p-type CNT-FETs show a lower dark current and a wider gate-voltage range of the OFF-state, which facilitates the measurement of the intrinsic photocurrent generated in nanotubes.

Figure 2 displays the photoconductivity excitation spectra for two CNT-FETs with the laser polarization parallel to the nanotube axis. The photocurrent as a function of photon energy shows a well-defined resonance at the excitation energy of 1.34 eV (Figure 2A) and 1.38 eV (Figure 2B), respectively. In addition, a weak peak appears at about 200 meV above the corresponding main resonance in both spectra. Height measurements by tapping mode AFM show individual nanotubes with diameter ~ 1.4 nm bridging the two electrodes in both devices. After examining the photoconductivity excitation spectra of a total of ~ 40 individual carbon nanotube incorporated CNT-FET devices in conjunction with AFM characterizations, we found that all samples with optical excitations in our laser energy range show a pair of peaks analogous to those displayed in Figure 2.¹⁴ We thus believe that the resonance and sideband peaks are correlated with each other and are both associated with the optical excitation of a single nanotube incorporated in the CNT-FETs. A strong depolarization effect on the photocur-

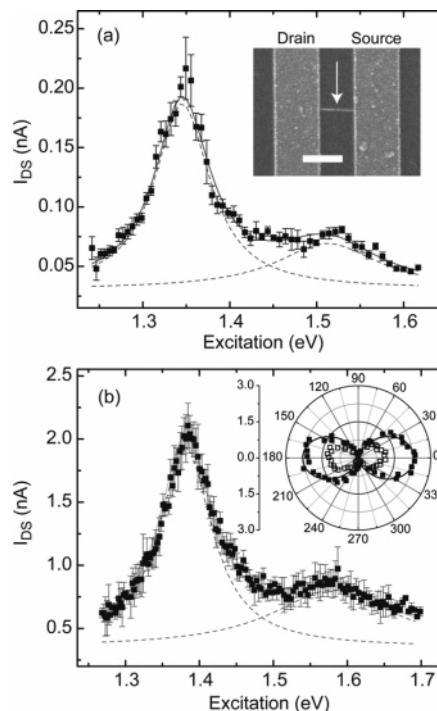


Figure 2. Photocurrent spectra of two CNT-FETs measured as a function of excitation photon energy. Co and Ti contacts are used in the two devices, respectively. $V_{ds} = -1$ V; $V_g = -0.5$ V. The displayed spectra are an average of several scans. The error bar denotes one-sigma error of the mean. Each of the spectra was fit by two Lorentzian peaks (dotted lines) superimposed on a constant baseline. The laser polarization direction is parallel to the nanotube orientation in the devices, which was determined by AFM or SEM images. A representative SEM image is shown in the inset of (a). The scale bar is $1 \mu\text{m}$. The inset in (b) shows the polarization dependence of the photocurrent of the second device measured at an excitation energy of 1.38 eV (solid square) and 1.58 eV (hollow square), respectively. The data obtained at 1.58 eV (sideband) are magnified by a factor of 3.

rent was clearly observed.¹⁵ As shown in the inset of Figure 2B, the resonance and sideband peak have the same polarization dependence, with essentially no photocurrent measured when the laser polarization is perpendicular to the CNT axis.

The resonance peaks in all of the measured photoconductivity spectra have a relatively symmetric line shape. To determine the peak positions of the resonance and sideband and their peak widths, we fit each spectrum with two Lorentzian peaks superimposed on a constant baseline. On average, the sideband peak is located ~ 190 meV above the resonance and has $\sim 30\%$ of the spectral weight of the resonance peak. The full width at half-maximum (fwhm) of the main resonance is ~ 90 meV. The sideband is broader, with a fwhm of ~ 180 meV.

Vis–near-IR absorption spectroscopy of our bulk nanotube material reveals three broad absorption bands at 0.73 , 1.38 , and 1.91 eV [see Supporting Information]. These three bands have been assigned to the transitions associated with the first (E_{11}^S) and second (E_{22}^S) pair of van Hove singularities (vHs) of the semiconducting CNTs, and the first vHs transition of the metallic nanotube in the CNT mixture, respectively.¹⁶ Statistically, the resonance peaks in our photoconductivity

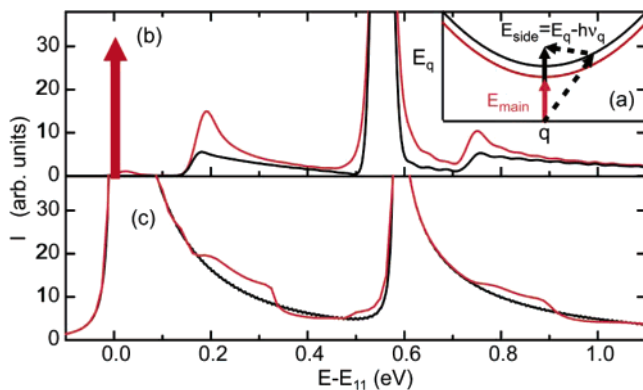


Figure 3. (a) Exciton band dispersion of the optically active exciton (red curve) and the dipole forbidden exciton (black curve). The dipole forbidden exciton is higher in energy than the optically active one at $q = 0$. (b) Absorption spectrum of the (17,0) nanotube calculated with (red) and without (black) exciton–phonon coupling for the exciton in a dielectric environment of $\epsilon = 4$. The zero energy here corresponds to the onset of the first optical active exciton, which has zero width and is shown by the vertical arrow. (c) Absorption spectrum of the same (17,0) tube assuming band-to-band absorption. The red curve is with, and the black curve without electron–phonon coupling.

experiments are centered at about 1.35 eV, which fits well with the energy expected for the E_{22}^S transition of CNTs with a mean diameter of ~ 1.3 nm.¹⁷

We performed tight-binding Bethe–Salpeter exciton calculations to evaluate the exciton–phonon interaction and its effect on the optical absorption of the nanotube.¹⁸ The exciton–phonon interaction was modeled by the Su–Schrieffer–Heeger (SSH) Hamiltonian.^{19,20} The noninteracting valence and conduction bands in a semiconducting nanotube are both doubly degenerate, which allows four degenerate pairs of electron–hole excitations. Coulomb interaction lifts the degeneracy partly. In Figure 3A we show schematically the dispersion of the optically active exciton and the doubly degenerate dipole-forbidden exciton at higher energy.²¹ In the absence of exciton–phonon coupling, the emission or absorption of a photon involves an optically active exciton of total wavevector q equal to the photon momentum, which is approximately $q = 0$. Exciton–phonon coupling, however, mixes the optically active exciton with the dipole forbidden “dark” exciton with finite q , so that the total exciton+phonon momentum is conserved. Of the two C–C stretching modes at the K and Γ points, the zone-boundary LO mode with energy of ~ 180 meV has the strongest electron–phonon coupling and mixes the two excitons.²²

Our calculations predict that the first optically active exciton corresponding to the E_{11} transition has a very small intrinsic width represented here by a delta function, while the second exciton has a finite width due to its coupling to the first quasi-particle band continuum (Figure 3B). Most importantly, the exciton–phonon coupling leads to the appearance of distinct sidebands similar to those appearing in the experimental spectra (Figure 2). As a result of the exciton splitting, the phonon sideband appears at an energy higher than the C–C stretching vibration (~ 180 meV) by an amount equal to the exciton splitting energy, i.e., the

energy difference between the optically allowed and dark exciton state at $q = 0$ (Figure 3A). For the second excitonic state in a dielectric environment with $\epsilon = 4$ (of SiO_2), our calculation predicts a splitting of ~ 10 meV and a $\sim 10\%$ spectral weight shift from the zero-phonon line (main peak) to the first phonon excitation peak. In contrast, the calculated band-to-band transition (band-gap excitation) spectra are characterized by long high energy tails as expected from the joint density of free particle states. In this case, inclusion of electron–phonon coupling does not lead to the appearance of well-defined sidebands (Figure 3C).

The calculated absorption spectrum shown in Figure 3B agrees well with the spectral features observed in the experimental measurements, reproducing the symmetric line shape of the main peak and the position of the sideband in the photoconductivity spectra at about 190 meV above the exciton transition. The good agreement not only illustrates the importance of exciton–phonon coupling on the optical properties of nanotubes but, more importantly, it provides strong support for the excitonic nature of nanotube optical excitation. In experiment as well as theory, the sideband peak is significantly wider than the main peak. Exciton dispersion is responsible for the broadening of the sideband, since a number of finite q -excitons contribute. The optical phonon dispersion is much smaller and its contribution to the sideband width is negligible.

Compared to the calculated optical absorption spectrum (Figure 3B), the experimentally obtained photocurrent spectra show a more intense sideband than that predicted by the calculation. An interesting possibility is that the additional spectral weight of the sideband might come from a direct contribution involving the second free-particle continuum of the nanotube. For a 1.3 nm diameter nanotube adsorbed on a silicon dioxide surface, calculations suggests that the energy of the second exciton state is a few hundred meV below the corresponding band-to-band transition.¹¹ The second quasi-particle band, therefore, might overlap the sideband (exciton+phonon state). That is, along with the exciton+phonon excitation, a band-to-band transition across the quasi-particle band-gap might occur in the same range, leading to a direct generation of free photocarriers in conduction and valence band, respectively. A study with wider range of laser frequency (not available to us) will be needed to verify this interesting possibility. In either case, however, the findings support the exciton interpretation of the main absorption peak.

In conclusion, we measured the laser photoconductivity excitation spectra of the second excited state of individual semiconducting carbon nanotubes that are incorporated as the channel of field-effect transistors. A well-defined resonance and a sideband feature at about 200 meV higher in energy were observed in the photocurrent spectra. Calculations show that the observed resonance arises from the excitonic transition associated with the second pair of van Hove singularities of the nanotubes, while the sideband is attributed to an exciton state with a simultaneous excitation of a C–C bond stretching phonon.

Acknowledgment. We acknowledge the expert technical assistance from Bruce Ek.

Supporting Information Available: Figure 1. Vis–NIR absorption spectrum of nanotubes dispersed in 1,2 dichloroethane. The region between the two vertical dashed lines indicates the laser excitation energy range in our experiments. This material is available free of charge via the Internet at <http://pubs.acs.org>.

References

- (1) O'Connell, M. J.; Bachilo, S. M.; Huffman, C. B.; Moore, V. C.; Strano, M. S.; Haroz, E. H.; Rialon, K. L.; Boul, P. J.; Noon, W. H.; Kittrell, C.; Ma, J.; Hauge, R. H.; Weisman, R. B.; Smalley, R. E. *Science* **2002**, 297, 593.
- (2) Bachilo, S. M.; Strano, M. S.; Kittrell, C.; Hauge, R. H.; Smalley, R. E.; Weisman, R. B. *Science* **2002**, 298, 2361.
- (3) Duesberg, G. S.; Loa, I.; Burghard, M.; Syassen, K.; Roth, S. *Phys. Rev. Lett.* **2000**, 85, 5436.
- (4) Freitag, M.; Martin, Y.; Misewich, J. A.; Martel, R.; Avouris, Ph. *Nano Lett.* **2003**, 3, 1067.
- (5) Misewich, J. A.; Martel, R.; Avouris, Ph.; Tsang, J. C.; Heinze, S.; Tersoff, J. *Science* **2003**, 300, 783.
- (6) Freitag, M.; Chen, J.; Tersoff, J.; Tsang, J.; Fu, Q.; Avouris, Ph. *Phys. Rev. Lett.* **2004**, 93, 076803.
- (7) Ando, T. *J. Phys. Soc. Jpn.* **1997**, 66, 1066.
- (8) Avouris, Ph. *MRS Bull.* **2004**, 29, 403.
- (9) Spataru, C. D.; Ismail-Beigi, S.; Benedict, L. X.; Louie, S. G. *Phys. Rev. Lett.* **2004**, 92, 077402.
- (10) Chang, E.; Bussi, G.; Ruini, A.; Molinari, E. *Phys. Rev. Lett.* **2004**, 92, 196401.
- (11) Perebeinos, V.; Tersoff, J.; Avouris, Ph. *Phys. Rev. Lett.* **2004**, 92, 257402.
- (12) Derycke, V.; Martel, R.; Appenzeller, J.; Avouris, Ph. *Nano Lett.* **2001**, 1, 453.
- (13) Balasubramanian, K.; Fan, Y.; Burghard, M.; Kern, K. *Appl. Phys. Lett.* **2004**, 84, 2400.
- (14) Most of the CNT-FETs studied in our experiment show a single resonance in the laser energy range between 1.24 eV to 1.77 eV. However, we could measure the sideband only in devices that have a resonance between 1.24 and 1.45 eV, because of the limitation of our laser excitation energy.
- (15) Ajiki, H.; Ando, T. *Physica B* **1994**, 201, 349.
- (16) Lebedkin, S.; Hannrich, F.; Skipa, T.; Kappes, M. *J. Phys. Chem. B* **2003**, 107, 1949.
- (17) Referring to the empirical Kataura plot in Weisman, R. B.; Bachilo, S. M. *Nano Lett.* **2003**, 3, 1235, the E_{22}^S of CNTs with a diameter of ~ 1.3 nm is approximately 1.35 eV. However, the exact energy of E_{22}^S is strongly dependent on the chirality.
- (18) Perebeinos, V.; Tersoff, J.; Avouris, Ph. *Phys. Rev. Lett.* **2005**, 94, 027402.
- (19) Su, W. P.; Schrieffer, J. R.; Heeger, A. J. *Phys. Rev. Lett.* **1979**, 42, 1698.
- (20) Su, W. P.; Schrieffer, J. R.; Heeger, A. J. *Phys. Rev. B* **1980**, 22, 2099.
- (21) Another singly degenerate state lies at lower energy than the allowed exciton at $q = 0$,¹¹ but this exciton does not mix with the $q = 0$ dipole allowed exciton by the exciton–phonon interaction.
- (22) Perebeinos, V.; Tersoff, J.; Avouris, Ph. cond-mat/0411021.

NL050227Y